Protein Science (2000), *9*:186–193. Cambridge University Press. Printed in the USA.

FOR THE RECORD

Amide proton hydrogen exchange rates for sperm whale myoglobin obtained from ^{15}N-^{1}H NMR spectra

SILVIA CAVAGNERO, YVES THÉRIAULT, SURINDER S. NARULA, H. JANE DYSON, AND PETER E. WRIGHT

Department of Molecular Biology and Skaggs Institute for Chemical Biology, The Scripps Research Institute, La Jolla, California 92037

(RECEIVED October 1, 1999; ACCEPTED November 2, 1999)

Abstract: The hydrogen exchange behavior of exchangeable protons in proteins can provide important information for understanding the principles of protein structure and function. The positions and exchange rates of the slowly-exchanging amide protons in sperm whale myoglobin have been mapped using ^{15}N-^{1}H NMR spectroscopy. The slowest-exchanging amide protons are those that are hydrogen bonded in the longest helices, including members of the B, E, and H helices. Significant protection factors were observed also in the A, C, and G helices, and for a few residues in the D and F helices. Knowledge of the identity of slowly-exchanging amide protons forms the basis for the extensive quench-flow kinetic folding experiments that have been performed for myoglobin, and gives insights into the tertiary interactions and dynamics in the protein.

Keywords: hydrogen exchange rate; proton-deuterium exchange; reference data

The exchange of interior labile protons with the protons of the solvent has long been advanced as the evidence for internal flexibility of the three-dimensional structure of proteins in solution (Linderström-Lang, 1955; Hvidt & Nielsen, 1966; Tanford, 1970). The exchange rates measured from the classical methods of infrared spectroscopy or tritium tracer experiments (Englander et al., 1972) were analyzed in terms of two-state "breathing modes" of the protein and apparent thermodynamic parameters were determined (Hvidt & Nielsen, 1966; Tanford, 1970; Richarz et al., 1979). With the development of NMR, exchange kinetics of individual amide protons in the proteins could be measured, for example, for basic pancreatic trypsin inhibitor and a group of related proteins (Wagner & Wüthrich, 1979). The hydrogen exchange data of proteins and nucleic acids have been interpreted in terms of solvent penetration and/or structural unfolding models (Englander & Kallenbach, 1984). Contributions to the exchange behavior of amide protons have been inferred from electrostatic effects (Delepierre et al., 1987), local unfolding (Kumar & Kallenbach, 1985), and local structural characteristics of proteins (Rashin, 1987).

Hydrogen exchange data are a necessary prerequisite for the study of protein folding by the quench-flow hydrogen exchange method (Roder et al., 1988; Udgaonkar & Baldwin, 1988), and the data obtained for the native protein can also give valuable information on local flexibility (Jeng & Dyson, 1995) and ligand binding sites (Jones et al., 1993; Williams et al., 1997) and may even provide a guide to the earliest-folding portions of the protein (Woodward, 1993). There have been a number of comprehensive recent studies of hydrogen exchange in a variety of native proteins, including ubiquitin (Briggs & Roder, 1992), cytochrome *c* (Milne et al., 1998), thioredoxin (Jeng & Dyson, 1995), barnase (Clarke et al., 1993), staphylococcal nuclease (Loh et al., 1993), Trp repressor (Finucane & Jardetzky, 1995), and lysozyme (Radford et al., 1992), as well as an evaluation of the stability of secondary and tertiary structure in unfolded and partly folded proteins (Chyan et al., 1993; Buck et al., 1994; Alexandrescu et al., 1996; Chamberlain & Marqusee, 1997). The interpretation of the results has been greatly enhanced by the publication of revised analyses of the effects of primary structure on hydrogen exchange rates (Bai et al., 1993; Connelly et al., 1993; Milne et al., 1998).

Myoglobin is a 153-residue heme protein that has been the focus for a great deal of structural and kinetic work for a period of many years. Its structure is the paradigm globin fold of eight helices, a number of which are stable even under mild denaturing conditions. A number of studies have utilized the relatively large number of slowly-exchanging amide protons in the carbon monoxide complex of myoglobin (MbCO) to determine the stabilities of helices (Hughson et al., 1990) and the rate of folding of the apoprotein (Jennings & Wright, 1993; Tsui et al., 1999). These studies relied on site-specific hydrogen exchange data that had been obtained from proton-only homonuclear NMR experiments; these results are summarized in the present paper. As a preface for more extensive and systematic examination of the folding kinetics of a series of myoglobin mutants, we have re-examined the hydrogen exchange of MbCO using ^{1}H-^{15}N heteronuclear single quantum co-

Reprint requests to: Dr. Peter E. Wright or Dr. H. Jane Dyson, Department of Molecular Biology MB2, The Scripps Research Institute, 10550 North Torrey Pines Road, La Jolla, California 92037; e-mail: wright@scripps.edu; dyson@scripps.edu.

herence (HSQC) spectra, which provide not only superior sensitivity and rapidity of acquisition, but also give improved dispersion of the resonances through the relatively wide dispersion in the ^{15}N dimension (Yao et al., 1997).

A total of 49 data points were recorded for MbCO at various times following the exchange of the protein into fully-deuterated buffer. The initial data point was acquired at 19 min after buffer exchange, and the next nine points were acquired back-to-back at intervals of 13 min. In the initial spectrum there were 89 cross peaks, and by the end of 24 h, 48 cross peaks of reasonable intensity remained, representing the maximum number of amide protons that could potentially be used as probes in a quench-flow hydrogen exchange experiment. This number is comparable to the 38 amide protons for which quench-flow kinetic data have been acquired (Jennings & Wright, 1993). The initial HSQC spectrum at the lowest time point is shown in Figure 1A. The final spectrum, taken at 126 days, is shown in Figure 1B. A total of 23 cross peaks remain, some of which have decayed in intensity to such a small extent that a reliable estimate of the exchange rate is difficult to make.

The cross peaks in the initial spectrum were assigned to individual amide protons according to published assignments at the same pH and temperature (Thériault et al., 1994). Cross peak heights were normalized at each time point with reference to an average of the cross peak heights of four well-resolved slowly-exchanging resonances, those of residues 29, 30, 32, and 111, which show negligible change in intensity over the full time course of the experiment. Exchange rates were computed using the program Templegraph, by nonlinear least-squares fitting to the cross peak heights as a function of time after the start of the exchange into D_2O. A similar procedure was followed for the proton-only experiments, where exchange rates were computed from data obtained from homonuclear two-dimensional (2D) correlation spectroscopy (COSY) spectra.

Table 1 shows the rates of exchange k_{exch} of 80 backbone amide protons and one indole side-chain amide, derived from well-resolved cross peaks in the ^{15}N-^{1}H HSQC spectrum, together with the intrinsic exchange rates k_{int} derived empirically according to the local amino acid sequence (Molday et al., 1972; Bai et al., 1993). These values were used to derive the protection factor PF at each backbone amide. In addition, overlapped cross peaks of slowly-exchanging amides are included in Table 1, with a notation as to the identity of the overlapped cross peaks. In some cases, the identity of the slowly-exchanging member of a pair of overlapped cross peaks can be inferred with some certainty, since one of the two is in a helical region of the protein, while the other is in an interhelical loop. For example, the amides of residues 99 and 133 are overlapped (Fig. 1A), but Ile99 is present on the border of the F and G helices in the MbCO structure and is surrounded by fast-exchanging amides, whereas Lys133 is toward the middle of the H helix and has slowly exchanging amides on either side. In addition, Lys133 amide was used in the quench-flow experiments (Jennings & Wright, 1993) and was unambiguously identified in the proton experiments (Table 1). The slowly-exchanging amide of this pair has therefore been assigned to Lys133, but with a notation in Table 1 that it is overlapped. In other cases, it is less clear which of the overlapped amides is likely to be the slowly-exchanging one, for example, Val114 and Leu115 cross peaks are overlapped, and it is not clear whether one or both of these amides contribute to the cross peak in Figure 1B. In these cases, the observed exchange rate is assigned to one of the overlapped resonances, but a notation is made in Table 1 that the rate could equally well apply to the other member of the pair or to both members. Finally, an exception occurs with the overlapped cross peak of Phe33 and Leu69. The raw intensity of this cross peak is approximately twice that of single-residue cross peaks in the same spectrum, an indication that both of these residues contribute intensity. In addition, the ^{1}H data, for which the overlap is relieved in this case due to the resolution of the Hα in the 2D COSY spectrum, show clear indications of slowly-exchanging amides for both Phe33 and Leu69 (Table 1). Both of these residues have therefore been included in Table 1. If the exchange rates of two residues with overlapped resonances are sufficiently well resolved in time, then it should be possible to fit the data to a multiple-exponential function and derive both exchange rates. Although this procedure was attempted in a number of cases, it was unsuccessful due to the errors in individual data points. A similar problem occurs in the case of some of the slower exchanging amides, for which the number of data points that contribute significantly to the determination of the exchange rate may be quite small; k_{exch} values slower than 10^{-7} s^{-1} ($-\log k_{exch} > 7$) are therefore not as precise as faster measured

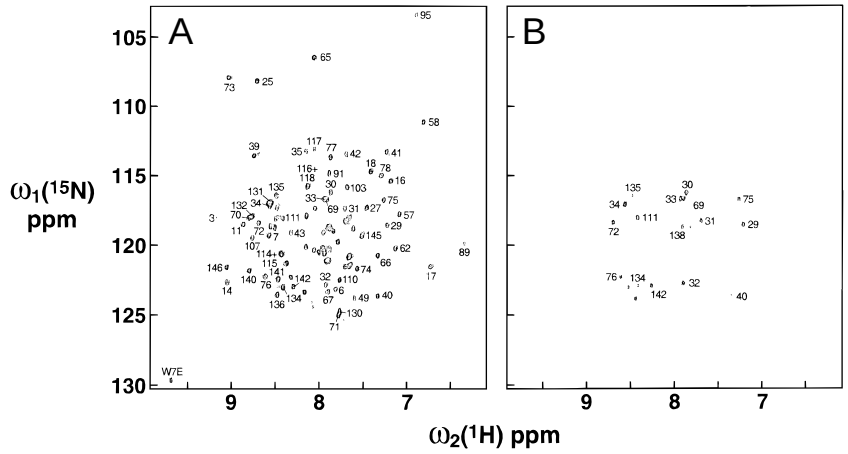

Fig. 1. ^{1}H–^{15}N HSQC spectra of MbCO showing (**A**) the earliest (19 min 2 s) and (**B**) the latest (126 days) time points after initiation of the hydrogen/deuterium exchange process.

Table 1. *Exchange rates and protection factors for MbCO (35 °C)*

Residue	Helix number	log k_{int}	^{15}N data[a]		^{1}H data	
			log k_{exch}	log PF	log k_{exch}	log PF
Ser3	A1	0.01	−2.9	2.9		
Glu6	A4	−0.49	−3.2	2.7		
Trp7	A5	−0.70	−3.9	3.2		
Trp7ϵ[b]			−2.9			
Gln8	A6	−0.20	−3.5(M131)[c]	3.3		
Leu9[d]	A7	−0.52	−4.4(A144)[c]	3.9		
Val10	A8	−1.05	−7.3	6.3	−7.0	5.9
Leu11	A9	−0.85	−6.3	5.4	−6.6	5.7
Val13	A11	−0.70	−3.2	2.5		
Trp14	A12	−0.70	−6.5	5.8	−6.9	6.2
Ala15	A13	−0.26	−3.6	3.4		
Lys16	A14	−0.72	−4.0	3.2	−4.2	4.0
Val17	A15	−0.72	−6.9	6.2	−6.8	6.1
Glu18	A16	−0.80	−5.1	4.3		
Gly25	B6	0.26	−3.6	3.9		
Asp27	B8	−0.25	−4.4	4.2		
Ile28	B9	−1.05	−6.4	5.3	−7.5	6.4
Leu29	B10	−0.96	−8.2	7.2	−7.1	6.1
Ile30	B11	−1.10	−8.5	7.4	−6.5	5.4
Arg31	B12	−0.3	−7.3(E54)[e]	−7.0		
Leu32	B13	−0.51	−8.3	7.8		
Phe33	B14	−0.60	−7.4(L69)[c]	6.8	−7.8	7.2
Lys34	B15	−0.13	−7.7	7.6		
Ser35	B16	0.34	−3.2	3.5		
His36	C1	0.05	−4.5	4.5		
Thr39	C4	−0.37	−5.7	5.3		
Leu40	C5	−0.52	−7.0	6.5		
Glu41	C6	−0.85	−3.6	2.8		
Lys42	C7	−0.34	−3.5	3.1		
Phe43	CD1	−0.27	−5.7	5.4	−5.5	5.2
Leu49	D1	−0.59	−3.0	2.4		
Glu54	D6	−0.66	O/L Arg31[e]			
Lys56	D8	−0.08	−3.3	3.2		
Ala57	D9	−0.03	−3.4	3.4	−3.8	3.8
Ser58	D10	0.22	−3.3	3.5		
Leu61	E4	−0.92	−4.4	3.5		
Lys62	E5	−0.4	−3.9	3.5		
Lys63	E6	−0.07	−4.3	4.2		
His64	E7	−0.13	−4.1	4.0		
Gly65	E8	0.26	−6.4	6.7	−6.5	6.8
Val66	E9	−0.68	−6.4	5.7	−6.7	6.0
Thr67	E10	−0.36	−3.4	3.0	−3.4	3.0
Val68	E11	−0.66	−6.6	6.0	−6.7	6.1
Leu69	E12	−0.85	−7.4(F33)[c]	6.6	−7.1	6.2
Thr70	E13	−0.43	−6.7	6.3	−6.9	6.5
Ala71	E14	0.05	−5.3	5.4	−5.2	5.3
Leu72	E15	−0.72	−7.3	6.6	−7.5	6.8
Gly73	E16	−0.09	−7.0	6.9	−6.9	6.8
Ala74	E17	0.02	−5.6	5.6	−5.5	5.5
Ile75	E18	−0.89	−7.6	6.7	−7.3	6.4
Leu76	E19	−0.96	−7.2	6.2	−6.6	5.6
Lys77	E20	−0.40	−5.8	5.4		
Lys78	E21	−0.07	−4.1	4.0		
Lys79	E22	−0.07	−4.4	4.3		
Glu85	EF	−0.66	−4.8	4.1		
Leu89	F4	−0.96	−3.0	2.0		
Ala90	F5	−0.36	−3.8	3.4	−3.7	3.4
Gln91	F6	−0.09	−3.2	3.1		
His93	F8	−0.05	−3.5	3.4	−3.7	3.6
Ala94	F9	−0.01	−4.7	4.7	−5.2	5.2

(*continued*)

Table 1. *Continued*

Residue	Helix number	log k_{int}	^{15}N data[a] log k_{exch}	^{15}N data[a] log PF	^{1}H data log k_{exch}	^{1}H data log PF
Thr95	F10	−0.22	−3.1	2.9	−3.5	3.3
Ile99	FG	−0.77	O/L Lys133[e]			
Tyr103	G4	−0.30	−5.2	4.9	−5.1	4.8
Leu104	G5	−0.68	−6.3	5.6		
Phe106	G7	−0.54	−4.8	4.3		
Ile107	G8	−0.82	−6.4	5.6	−6.1	5.3
Ser108	G9	−0.01	−3.7	3.7		
Glu109	G10	−0.36	−4.2	3.9		
Ala110	G11	−0.30	−5.6	5.3		
Ile111[f]	G12	−0.89	<-8	>7		
Ile112	G13	−1.10	O/L Phe138[c]			
His113	G14	−0.48	−5.3	4.8		
Val114	G15	−0.70	−6.7(L115)[c]	6.0		
Leu115	G16	−0.85	O/L Val114[c]			
His116	G17	−0.46	O/L Arg118[c]			
Ser117	G18	0.36	−2.9	3.3		
Arg118	G19	0.23	−3.5(H116)[c]	3.7		
Gln128	H5	−0.09	−3.0	2.9		
Ala130	H7	0.02	−3.2	3.2	−3.7	3.7
Met131	H8	−0.16	O/L Gln8[c]			
Asn132	H9	0.45	−4.3	4.7	−4.5	4.9
Lys133	H10	0.13	−5.1(I99)[e]	5.4	−5.2	5.3
Ala134	H11	−0.03	−7.1	7.1	−7.3	7.3
Leu135	H12	−0.72	−7.1	6.4		
Glu136	H13	−0.85	−7.0	6.2		
Leu137	H14	−0.89	−6.7	5.8		
Phe138	H15	−0.60	−6.7(I112)[c]	6.1	−6.9	6.3
Arg139	H16	−0.01	−7.0	7.0		
Lys140	H17	0.03	−5.8	5.8		
Asp141	H18	−0.33	−5.6	5.3		
Ile142	H19	−1.05	−7.8	6.7	−7.1	6.1
Ala143	H20	−0.38	−6.4	6.0	−6.3	5.9
Ala144	H21	−0.15	O/L Leu9[c]		−3.8	3.7
Lys145	H22	−0.19	−4.2	4.0	−4.3	4.1
Tyr146	H23	−0.30	−4.5	4.2		
Lys147	H24	−0.14	−2.8	2.6		
Leu149	H26	−0.89	−3.3	2.4		

[a]The H/D exchange kinetic data range in accuracy from ±4% for well-determined data to ±50% for badly determined data, particularly for the slowest-exchanging amide protons. These values were estimated from the standard error of the least-squares fits expressed as relative standard deviation. All exchange rates in this table are in s^{-1}.

[b]Side-chain indole NH.

[c]Exchange rates that are ambiguous due to overlap of the ^{15}N–^{1}H cross peak in the HSQC spectrum, but for which either member of the pair (or both) could contribute to the observed exchange behavior. In the case of Phe33 and Leu69, it appears that the very slow exchange rate applies to both residues, since the cross peak in the long-time spectra has an intensity approximately twice that of a single resonance, and the ^{1}H data were able to distinguish them. For the remaining overlapped cross peaks of the HSQC spectrum, only one of the residues has been identified, but the overlapping residue has been noted. In the case of Ala144–Leu9, the ^{1}H data indicate that the exchange rate applies to Ala144, but Leu9 was identified in previous work (Jennings & Wright, 1993) as a slowly-exchanging amide proton.

[d]Residues in bold were identified as slowly-exchanging in the quench-flow study of apomyoglobin folding (Jennings & Wright, 1993).

[e]Exchange rates that are ambiguous due to overlap of the ^{15}N–^{1}H cross peak in the HSQC spectrum, but which can be assigned with confidence to the residue shown. These pairs of residues are: Arg31–Glu54 and Lys133–Ile99.

[f]The exchange rates for the Ile111 amide proton were too slow to be measured accurately within the experimental timescale of this work. This residue was also one of those used to normalize the data before curve fitting. Therefore, only estimated upper limit value of k_{ex} and lower limit value of PF are shown in the table.

rates. At the other extreme, exchange rates faster than 10^{-3} s^{-1} were very difficult to determine precisely, again due to the paucity of data points. The exchange rates obtained from the ^{1}H data are also included in Table 1. It is noticeable that these values in the main agree very well with the more comprehensive set of data obtained from the ^{15}N-^{1}H spectra.

The exchange rate is plotted as a function of residue number in Figure 2, which illustrates that the slowly-exchanging amides are localized in the helices. In particular, the slowest rates of exchange are seen in the B, E, and H helices, which are thereby identified as the most stable parts of the holomyoglobin molecule. These results form an interesting contrast to the locations of secondary structure in the earliest folding intermediate of apomyoglobin (Jennings & Wright, 1993) and in the equilibrium molten globule that corresponds to it (Eliezer et al., 1998). The earliest folded secondary structure is detected in the A, G, and H helices, and the B and E helices fold later, on an ms time scale (Jennings & Wright, 1993). These differences are doubtless due to the presence of the heme, which clearly stabilizes the structure of the helices that contact it. This stabilization is seen in particular for the F helix, which in apomyoglobin appears to be in a state of conformational exchange on a millisecond timescale, giving rise to broadened resonances (Eliezer & Wright, 1996). By contrast, in the holoprotein, the F helix is sufficiently stable to protect some amide protons from exchange (Table 1; Fig. 2).

The presence of the heme group complicates a consideration of the exchange mechanisms of MbCO. A protein of the size of myoglobin is expected to undergo exchange via an EX2 mechanism, i.e., via local rather than global unfolding (Hvidt & Nielsen, 1966). Under these circumstances, the groups exposed by the same local opening motion can be identified by their relationship to each other along lines of unit slope in a plot of $\log(k_{exch})$ against $\log(k_{int})$ (Wand et al., 1986; Qiwen et al., 1987). Such a plot is shown in Figure 3A for MbCO. Each of the helices contains residues associated with a number of lines. The helices with the majority of their residues at the bottom of the figure (slowest exchanging) are the B, E, and H helices. The C-helix also has three residues in this region. By contrast, all of the residues in the D- and F-helices are present at the top of the figure, indicating that the opening motion that results in exchange for these helices is rapid and complete. Amide protons in the loops that connect the helices, as well as several amides in the D- and F-helices, exchange too rapidly to measure by the techniques used here. On the other hand, a majority of the amides of the B-, E-, G-, and H-helices are represented in Table 1, and those that are missing from Figure 3A are either overlapped or at the ends of the helices where they make the transition to solvent-exposed loops.

A similar pattern of exchange protection is seen for each helix. Figure 3B shows the data for the B-helix alone. The slowest-exchanging amides are in the center of the helix; residues 29–34 appear to be connected by a line of unit slope, suggesting that their exchange is correlated and occurs through the same motion of the structure. The faster-exchanging residues 25, 27, and 35 also lie on a line, although it is probably coincidental that the N- and C-terminal parts of the helix appear on the same line. The increased exchange rates near the termini of helix B and many of the other helices are an indication that the dynamic fraying is occurring in these regions.

Another important factor in the exchange process is the degree to which the amide is sequestered from solvent by a surrounding hydrophobic medium. Those residues with the slowest exchange rates according to Figure 3 are also those which are sequestered from solvent. This is illustrated in Figure 4. The B-helix (Fig. 4A) is rather uniformly well protected at the center, due to contacts with the D-helix (toward the top of the figure) and the G-helix (directly below the B-helix), as well as extensive heme contacts (behind the B-helix). By contrast, the G- and H-helices (Fig. 4B) are less uniformly protected in the center of the helix. In particular, the G-helix (Fig. 4B), as well as the E-helix (not shown), shows a periodicity that indicates that only those amides that are buried in the core of the protein are significantly protected: the protection of the solvent-exposed amides is quite low in some cases.

At the level of individual helices, the protection of the amides is understandable in terms of local unfolding reactions, as shown by the relationships in Figure 3 and illustrated in Figure 4. Such locally cooperative hydrogen exchange in helical segments has been observed in a number of proteins (Wagner & Wüthrich, 1982; Kuwajima & Baldwin, 1983; Wand et al., 1986; Louie et al., 1988). The motions that give rise to these patterns of exchange are crucially dependent on the local amino acid sequence. Thus, despite the similarities in the structures of myoglobin and the plant-derived homologue leghemoglobin, there are significant differences in their exchange behavior; for example, the A-helix is labile in leghemoglobin (Morikis & Wright, 1996) but quite stable in MbCO. These stability differences are manifest in differences in the folding pathway, as shown by quench-flow hydrogen exchange measurements (Jennings & Wright, 1993; C. Nishimura, S. Prytulla, H.J. Dyson, P.E. Wright, in prep.). Heme proteins, such as myoglobin and leghemoglobin, are particularly amenable to study by quench-flow methods, due to the simplicity of the folding behavior, as well as to the stabilization of the final folded state by the heme, which allows detailed analysis of partly deuterated folding intermediates by NMR.

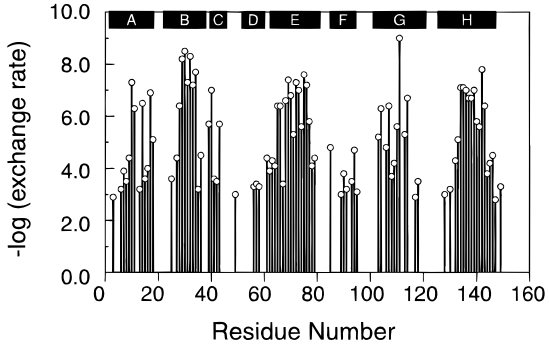

Fig. 2. Logarithmic plot of the experimentally observed hydrogen/deuterium exchange rates (k_{exch}) for MbCO after transfer of the protein into D_2O medium. The exchange rate of the Trp^7 ϵ–side-chain proton is not shown in this figure (see Table 1).

Materials and methods: *Sample preparation*: Recombinant ^{15}N-labeled sperm whale apomyoglobin (apoMb) was prepared as described previously (Jennings et al., 1995; Eliezer et al., 1997). The reconstitution of apoMb with heme was performed according to published procedures (Jennings et al., 1995), and the holoprotein was dissolved in 50 mM potassium phosphate in H_2O (pH 5.6). The carbon monoxide complex of the reduced form of myoglobin was prepared under anaerobic conditions in a CO-saturated atmosphere. All the buffers and solutions used were carefully CO-saturated prior to use. A threefold excess of sodium dithionite in 0.1 M NaOH was added to the myoglobin solution (about 0.3 mL) with stirring. Excess dithionite and hemin were removed during the following step, which marked the beginning of the hydrogen-deuterium exchange process. The solution was rapidly passed through a small G-15 gel filtration column (capacity

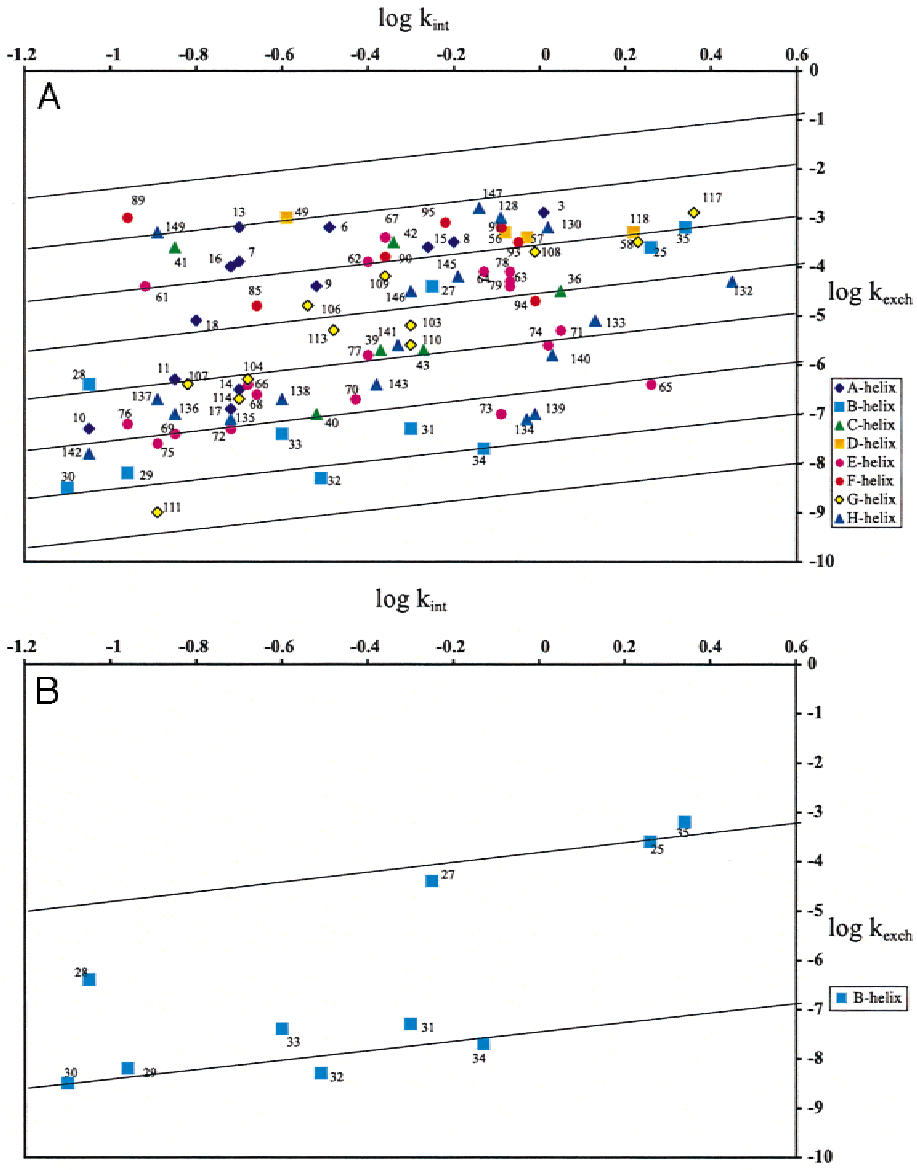

Fig. 3. A: Plot of the logarithm of the intrinsic exchange rate (k_{int}) against the logarithm of the measured exchange rate (k_{exch}) for MbCO. The data are differentiated according to which of the eight helices are closest (residues in loops are included in the nearest helix for clarity). Oblique lines with unit slope are drawn for illustrative purposes, and the entries are labeled with the residue number from the MbCO sequence. **B:** Selection of the data from **A** showing the points for the B-helix only. The two oblique lines represent estimates obtained by eye for the best fit of a line of unit slope to points at the ends of the helix (upper line) and in the middle of the helix (lower line).

3 mL) that had been pre-equilibrated in 50 mM potassium phosphate in D_2O (pH* 5.2). pH* denotes the apparent pH-meter reading. Corrected for the deuterium isotope effect, the pD value is 5.6. The column eluate was collected directly into the NMR tube under a CO-saturated atmosphere. The time corresponding to protein loading on the column marked the beginning of the hydrogen/deuterium exchange process. The overall dead time of the experiment, spanning from sample loading on the column to the beginning of NMR data acquisition, was 19 min and 2 s. Hydrogen/deuterium exchange experiments were carried out under temperature-controlled conditions (35 ± 0.1 °C) in the magnet. Initially, data were collected every few minutes, then every few hours until the end of the first eight days. Subsequent data were collected at daily or weekly intervals to obtain information about the hydrogen/deuterium exchange rates of slowly exchanging amide protons. The NMR sample was kept in a thermostated bath at 35 ± 1 °C while undergoing exchange outside the magnet. The range of collected time points was from 19 min to 126 days.

Preparation of the unlabeled samples of sperm whale MbCO used to obtain the proton-only data followed established protocols (Dalvit & Wright, 1987)

NMR spectroscopy: The time course of hydrogen/deuterium exchange was followed for the ^{15}N-labeled samples by recording

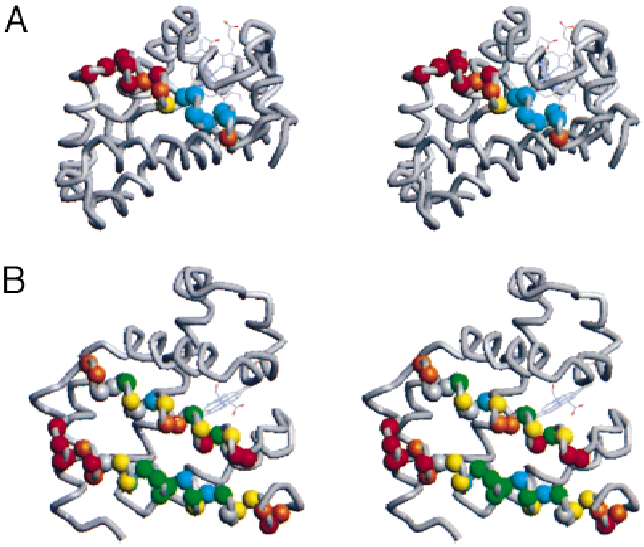

Fig. 4. Stereo representations of the backbone structure of MbCO showing the position of amides in (**A**) the B-helix and (**B**) the G- and H-helices. Red spheres indicate amides with exchange rates too fast to measure in the H-D experiment; orange, amides approximately within the top two segments of Figure 3A (delineated by the oblique lines); yellow, within the next segment; green, within the next segment; and blue, within the bottom two segments. Grey spheres indicate those amides that are ambiguous due to overlap (Table 1). Coordinates were derived from the X-ray structure of MbCO (Kuriyan et al., 1986).

sensitivity-enhanced ^{15}N-^{1}H-HSQC NMR experiments with gradient coherence selection (Kay et al., 1992; Zhang et al., 1994) on a Bruker AMX-500 spectrometer operating at 500.13 MHz and equipped with a ^{1}H/^{13}C/^{15}N triple-resonance probe. Suppression of the residual HDO signal was achieved by the solvent-flipback pulse sequence (Grzesiek & Bax, 1993). All spectra were recorded with identical acquisition parameters. Each spectrum was collected as a 512 × 64 complex point matrix covering spectral widths of 4,032 and 1,667 Hz in ω_2 and ω_1, respectively. The total measuring time for each HSQC experiment was 12 min 52 s. Temperature was 35 ± 0.1 °C. Given the standard correction by +0.4 pH units due to the isotope effect in D_2O, the NMR resonances of this study (in buffered D_2O at pH* 5.2) have been directly related to the known assignments for MbCO in buffered protonated medium at pH 5.6 (Thériault et al., 1994; Jennings et al., 1995). These were based on data recorded under the same experimental conditions, except for the medium, which was protonated and at pH 5.6. Data were processed and visualized on an SGI workstation with the NMRpipe and NMRdraw software packages (Delaglio et al., 1995). To attain the maximum resolution in the spectra, an 18°-shifted sine-bell window function was applied to the time-domain data in the ω_2 dimension, and linear prediction was employed. A 45° shifted sine-bell window function was used in ω_1. The final size of the spectrum was extended to 1,024 × 512 real points by zero-filling. Data were analyzed by the NMRview software (Johnson & Blevins, 1994).

The ^{1}H data were obtained by acquiring COSY spectra at times between 0.68 and 4,000 h after transfer to deuterated buffer. The pD of the sample was 5.6 and the temperature was kept constant, both inside and outside the probe, at 35 °C.

Data analysis: For the ^{15}N-labeled sample, hydrogen/deuterium exchange was followed by peak intensities in the HSQC spectra collected at each time point. Peak intensities within each spectrum were normalized to the average of four long-lived cross peaks. Data were fitted by a nonlinear least-squares algorithm to a single exponential decay with the Kaleidagraph package (Synergy Software, Reading, Pennsylvania) or with the Templegraph package (Mihalisin Associates, Maple Glen, Pennsylvania). Uncertainties for the hydrogen/deuterium exchange rate constants derived from experimental data (k_{exch}) were estimated from the standard deviations obtained from the covariance matrix of the curve-fitting algorithm. Protection factors (PF) were calculated from k_{exch} and k_{int} (PF = k_{exch}/k_{int}). k_{int} denotes the intrinsic hydrogen/deuterium rate constant of the residue of interest within a short reference peptide. Values were calculated by known methods (Englander & Poulsen, 1969; Englander et al., 1979) and were corrected for the effect of local sequence differences (Molday et al., 1972; Bai et al., 1993), and experimental pH and temperature (Englander & Poulsen, 1969; Englander et al., 1979; Connelly et al., 1993).

Acknowledgments: We thank Gerard Kroon for help with analysis of the data. Mark Chiu acquired some preliminary ^{15}N data on amide exchange in MbCO. This work was supported by grants GM34909 (P.E.W.) and GM57374 (H.J.D.) from the National Institutes of Health, and, in part, by the Wills Foundation (S.C.).

References

Alexandrescu AT, Dames SA, Wiltscheck R. 1996. A fragment of staphylococcal nuclease with an OB-fold structure shows hydrogen-exchange protection factors in the range reported for "molten globules." *Protein Sci 5*:1942–1946.

Bai Y, Milne JS, Mayne L, Englander SW. 1993. Primary structure effects on peptide group hydrogen exchange. *Proteins 17*:75–86.

Briggs MS, Roder H. 1992. Early hydrogen-bonding events in the folding reaction of ubiquitin. *Proc Natl Acad Sci USA 89*:2017–2021.

Buck M, Radford SE, Dobson CM. 1994. Amide hydrogen exchange in a highly denatured state. Hen egg-white lysozyme in urea. *J Mol Biol 237*:247–254.

Chamberlain AK, Marqusee S. 1997. Touring the landscapes: Partially folded proteins examined by hydrogen exchange. *Structure 5*:859–863.

Chyan C-L, Wormald C, Dobson CM, Evans PA, Baum J. 1993. Structure and stability of the molten globule state of guinea pig α-lactalbumin: A hydrogen exchange study. *Biochemistry 32*:5681–5691.

Clarke J, Hounslow AM, Bycroft M, Fersht AR. 1993. Local breathing and global unfolding in hydrogen exchange of barnase and its relationship to protein folding pathways. *Proc Natl Acad Sci USA 90*:9837–9841.

Connelly GP, Bai Y, Jeng M-F, Englander SW. 1993. Isotope effects in peptide group hydrogen exchange. *Proteins 17*:87–92.

Dalvit C, Wright PE. 1987. Assignment of resonances in the ^{1}H nuclear magnetic resonance spectrum of the carbon monoxide complex of sperm whale myoglobin by phase-sensitive two-dimensional techniques. *J Mol Biol 194*:313–327.

Delaglio F, Grzesiek S, Vuister GW, Guang Z, Pfeifer J, Bax A. 1995. NMRPipe: A multidimensional spectral processing system based on UNIX pipes. *J Biomol NMR 6*:277–293.

Delepierre M, Dobson CM, Karplus M, Poulsen FM, States DJ, Wedin RE. 1987. Electrostatic effects and hydrogen exchange behaviour in proteins. The pH dependence of exchange rates in lysozyme. *J Mol Biol 197*:111–130.

Eliezer D, Jennings PA, Dyson HJ, Wright PE. 1997. Populating the equilibrium molten globule state of apomyoglobin under conditions suitable for characterization by NMR. *FEBS Lett 417*:92–96.

Eliezer D, Wright P. 1996. Is apomyoglobin a molten globule? Structural characterization by NMR. *J Mol Biol 263*:531–538.

Eliezer D, Yao J, Dyson HJ, Wright PE. 1998. Structural and dynamic characterization of partially folded states of myoglobin and implications for protein folding. *Nature Struct Biol 5*:148–155.

Englander JJ, Calhoun DB, Englander SW. 1979. Measurement and calibration of peptide group hydrogen exchange by ultraviolet spectroscopy. *Analyt Biochem 92*:517–524.

Englander SW, Downer NW, Teitelbaum H. 1972. Hydrogen exchange. *Ann Rev Biochem 41*:903–924.

Englander SW, Kallenbach NR. 1984. Hydrogen exchange and structural dynamics of proteins and nucleic acids. *Quart Rev Biophys 16*:521–655.

Englander SW, Poulsen A. 1969. Hydrogen-tritium exchange of the random chain polypeptide. *Biopolymers 7*:379–393.

Finucane MD, Jardetzky O. 1995. Mechanism of hydrogen-deuterium exchange in *trp* repressor studied by ^{1}H-^{15}N NMR. *J Mol Biol 253*:576–589.

Grzesiek S, Bax A. 1993. The importance of not saturating H_2O in protein NMR. Application to sensitivity enhancement and NOE measurements. *J Am Chem Soc 115*:12593–12594.

Hughson FM, Wright PE, Baldwin RL. 1990. Structural characterization of a partly folded apomyoglobin intermediate. *Science 249*:1544–1548.

Hvidt A, Nielsen SO. 1966. Hydrogen exchange in proteins. *Adv Protein Chem 21*:287–339.

Jeng M-F, Dyson HJ. 1995. Comparison of the hydrogen exchange behavior of reduced and oxidized *Escherichia coli* thioredoxin. *Biochemistry 34*:611–619.

Jennings PA, Stone MJ, Wright PE. 1995. Overexpression of myoglobin and assignment of the amide, Cα and Cβ resonances. *J Biomol NMR 6*:271–276.

Jennings PA, Wright PE. 1993. Formation of a molten globule intermediate early in the kinetic folding pathway of apomyoglobin. *Science 262*:892–896.

Johnson BA, Blevins RA. 1994. NMRView: A computer program for the visualization and analysis of NMR data. *J Chem Phys 29*:1012–1014.

Jones DNM, Bycroft M, Lubienski MJ, Fersht AR. 1993. Identification of the barstar binding site of barnase by NMR spectroscopy and hydrogen-deuterium exchange. *FEBS Lett 331*:165–172.

Kay LE, Keifer P, Saarinen T. 1992. Pure absorption gradient enhanced heteronuclear single quantum correlation spectroscopy with improved sensitivity. *J Am Chem Soc 114*:10663–10665.

Kumar NV, Kallenbach NR. 1985. Hydrogen exchange of individual amide protons in the F helix of cyanometmyoglobin. *Biochemistry 24*:7658–7662.

Kuriyan J, Wilz S, Karplus M, Petsko GA. 1986. X-ray structure and refinement of carbon-monoxy (Fe II)-myoglobin at 1.5 Å resolution. *J Mol Biol 192*:133–154.

Kuwajima K, Baldwin RL. 1983. Nature and locations of the most slowly exchanging peptide NH protons in residues 1 to 19 of ribonuclease S. *J Mol Biol 169*:281–297.

Linderström-Lang K. 1955. Deuterium exchange between peptides and water. *Chem Soc Spec Publ 2*:1–20.

Loh SN, Prehoda KE, Wang J, Markley JL. 1993. Hydrogen exchange in unligated and ligated staphylococcal nuclease. *Biochemistry 32*:11022–11028.

Louie G, Englander JJ, Englander SW. 1988. Salt, phosphate and the Bohr effect at the hemoglobin beta chain C terminus studied by hydrogen exchange. *J Mol Biol 201*:765–772.

Milne JS, Mayne L, Roder H, Wand AJ, Englander SW. 1998. Determinants of protein hydrogen exchange studied in equine cytochrome *c*. *Protein Sci 7*:739–745.

Molday RS, Englander SW, Kallen RG. 1972. Primary structure effects on peptide group hydrogen exchange. *Biochemistry 11*:150–158.

Morikis D, Wright PE. 1996. Hydrogen exchange in the carbon monoxide complex of soybean leghemoglobin. *Eur J Biochem 237*:212–220.

Qiwen W, Kline AD, Wüthrich K. 1987. Amide proton exchange in the α-amylase polypeptide inhibitor tendamistat studied by two-dimensional ^{1}H nuclear magnetic resonance. *Biochemistry 26*:6488–6493.

Radford SE, Buck M, Topping KD, Dobson CM, Evans PA. 1992. Hydrogen exchange in native and denatured states of hen egg-white lysozyme. *Proteins 14*:237–248.

Rashin AA. 1987. Correlation between calculated local stability and hydrogen exchange rates in proteins. *J Mol Biol 198*:339–349.

Richarz R, Sehr P, Wagner G, Wüthrich K. 1979. Kinetics of the exchange of individual amide protons in the basic pancreatic trypsin inhibitor. *J Mol Biol 130*:19–30.

Roder H, Elöve GA, Englander SW. 1988. Structural characterization of folding intermediates in cytochrome *c* by H-exchange labelling and proton NMR. *Nature 335*:700–704.

Tanford C. 1970. Protein denaturation. Part C. Theoretical models for the mechanism of denaturation. *Adv Protein Chem 24*:1–95.

Thériault Y, Pochapsky TC, Dalvit C, Chiu ML, Sligar SG, Wright PE. 1994. ^{1}H and ^{15}N resonance assignments and secondary structure of the carbon monoxide complex of sperm whale myoglobin. *J Biomol NMR 4*:491–504.

Tsui V, Garcia C, Cavagnero S, Siuzdak G, Dyson HJ, Wright PE. 1999. Quench-flow experiments combined with mass spectrometry show apomyoglobin folds through an obligatory intermediate. *Protein Sci 8*:45–49.

Udgaonkar JB, Baldwin RL. 1988. NMR evidence for an early framework intermediate on the folding pathway of ribonuclease A. *Nature 335*:694–699.

Wagner G, Wüthrich K. 1979. Structural interpretation of the amide proton exchange in the basic pancreatic trypsin inhibitor and related proteins. *J Mol Biol 134*:75–94.

Wagner G, Wüthrich K. 1982. Amide proton exchange and surface conformation of the basic pancreatic trypsin inhibitor in solution. Studies with two-dimensional nuclear magnetic resonance. *J Mol Biol 160*:343–361.

Wand AJ, Roder H, Englander SW. 1986. Two-dimensional ^{1}H NMR studies of cytochrome *c*: Hydrogen exchange in the N-terminal helix. *Biochemistry 25*:1107–1114.

Williams DC, Rule GS, Poljak RJ, Benjamin DC. 1997. Reduction in the amide hydrogen exchange rates of an anti-lysozyme Fv fragment due to formation of the Fv-lysozyme complex. *J Mol Biol 270*:751–762.

Woodward C. 1993. Is the slow-exchange core the protein folding core? *Trends Biochem Sci 18*:359–360.

Yao J, Dyson HJ, Wright PE. 1997. Chemical shift dispersion and secondary structure prediction in unfolded and partly folded proteins. *FEBS Lett 419*:285–289.

Zhang O, Kay LE, Olivier JP, Forman-Kay JD. 1994. Backbone ^{1}H and ^{15}N resonance assignments of the N-terminal SH3 domain of drk in folded and unfolded states using enhanced-sensitivity pulsed field gradient NMR techniques. *J Biomol NMR 4*:845–858.